energies

MDPI

Article

Core-Loss Analysis of Linear Magnetic Gears Using the Analytical Method

Jeong-In Lee [1], Kyung-Hun Shin [2], Tae-Kyoung Bang [1], Kyong-Hwan Kim [3], Key-Yong Hong [3] and Jang-Young Choi [1,*]

[1] Department of Electrical Engineering, Chungnam National University, Daejeon 34134, Korea; lji477@cnu.ac.kr (J.-I.L.); bangtk77@cnu.ac.kr (T.-K.B.)
[2] Department of Power System Engineering, Chonnam National University, Yeosu 59626, Korea; kshin@chonnam.ac.kr
[3] Offshore Plant Research Division, Korea Research Institute of Ships and Ocean Engineering, Daejeon 34103, Korea; khong@kriso.re.kr (K.-H.K.); kkim@kriso.re.kr (K.-Y.H.)
* Correspondence: choi_jy@cnu.ac.kr

Abstract: In this study, analysis of core-loss occurring in the magnetic flux modulation core of a linear magnetic gear and the core of each mover is presented, using an analytical method. Losses in electric machines were generally calculated and analyzed using the finite element method (FEM). However, in the case of core-loss, the exact loss value could not be calculated using FEM data. Therefore, we considered the harmonic component of the air-gap magnetic flux density waveform with the modified Steinmetz equation, and performed a more accurate core-loss analysis with magnetic behavior analysis. Thus, we performed a calculated core-loss characteristic comparison with the FEM and the modified Steinmetz equation.

Keywords: core loss; finite element method (FEM); linear magnetic gear; linear machines; permanent magnet machines

Citation: Lee, J.-I.; Shin, K.-H.; Bang, T.-K.; Kim, K.-H.; Hong, K.-Y.; Choi, J.-Y. Core-Loss Analysis of Linear Magnetic Gears Using the Analytical Method. *Energies* **2021**, *14*, 2905. https://doi.org/10.3390/en14102905

Academic Editor: Nick Baker

Received: 19 January 2021
Accepted: 13 May 2021
Published: 18 May 2021

1. Introduction

Gears are mechanical devices that transmit rotation or power through two or more axes. Gears are used in various fields such as automobile systems, generators, and systems that require speed acceleration/deceleration, owing to their high torque and efficiency [1,2]. However, mechanical gears are driven through the physical engagement of teeth. Owing to such physical contact, efficiency is reduced because of the damage and loss of gears during long-time operation or system overload. In addition, they yield noise and vibration due to friction and require regular maintenance using lubricating oil [3]. Therefore, in order to compensate for the problems of mechanical gears, using permanent magnets of Neodium (NdFeB) and Samarium Cobalt (Sm_2Co_{17}), which are excellent in recent high magnetic energy and temperature characteristics, various studies propose non-contact magnetic gears that are capable of transmitting power. Magnetic gears, unlike mechanical gears, can minimize loss, noise, vibration, and dust, due to contactless operation using permanent magnets rather than teeth, and can be used semi-permanently by preventing damage to the gears through system overload slip [4,5]. In addition, since there is no physical contact, it has the advantage of not requiring regular maintenance. In general, the loss of a permanent magnet machines includes core-loss in the core, eddy current loss in the permanent magnet, copper loss in the coil, and friction loss due to mechanical contact. However, linear magnetic gears do not have coils, and due to non-contact driving, copper loss and friction loss do not occur, but core-loss and eddy current loss occur.

An active research on the core-loss analysis of permanent magnet machine began with the model proposed by Steinmetz. Since then, many researchers proposed a more advanced method of core-loss analysis. In most paper, core-loss analysis is computed or analyzed

through FEM to accurately identify the convenience and distribution of the analysis. However, in core-loss analysis using the FEM, the core-loss coefficient is inaccurate, and only the maximum value of the magnetic flux density is used [6]. In addition, it is difficult to accurately analyze the core-loss because the rotating magnetic field is not considered, and the magnetic field behavior analysis is very important for core-loss analysis. As for the core-loss, the magnitude of the loss varies, depending on the magnetic field behavior. Additionally, since the magnetic flux density generated by harmonics increases the core-loss, it is necessary to perform an accurate core-loss analysis in consideration of the harmonics and the magnetic field behavior for accurate core-loss prediction.

Therefore, in this study, the normal component magnetic flux density and tangential component of each region was obtained through FEM, after deriving the core-loss coefficient function of the equation through a modified Steinmetz equation. This was carried out using curve fitting based on the core-loss data provided by the core manufacturer and the magnetic flux density was analyzed by Fast Fourier Transform (FFT). The harmonic analysis and components of the linear magnetic gear magnetic flux density waveform were considered, and the characteristics of the rotating magnetic field and the alternating magnetic field were analyzed through magnetic field behavior analysis. Therefore, a more accurate core-loss analysis was performed than the core-loss analysis of FEM, and the proposed core-loss analysis process is shown in Figure 1; as shown below.

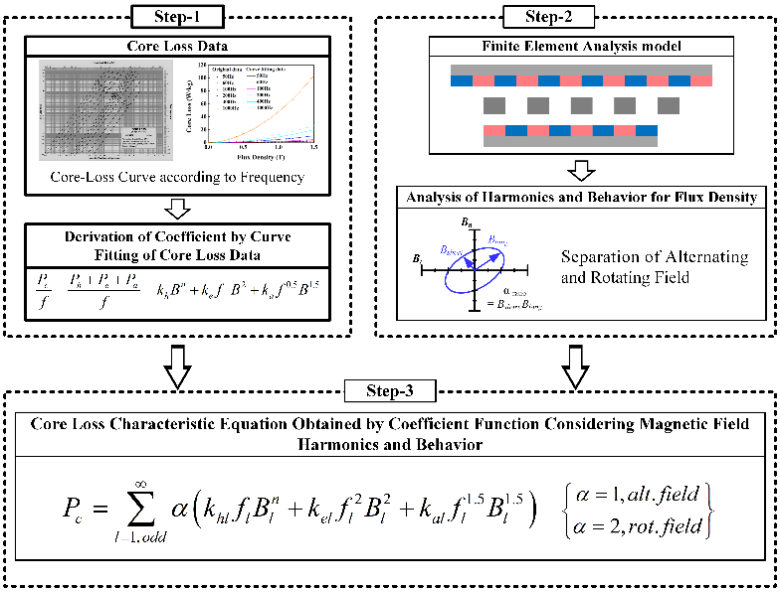

Figure 1. Proposed core-loss analysis flow chart.

- Derivation of the core-loss curve fitting and core-loss coefficients according to the frequency of the core provided by the manufacturer.
- Analysis of magnetic flux density and magnetic field behavior according to the core region.
- Calculation of core-loss using modified Steinmetz equation of linear magnetic gears, taking into account magnetic field behavior and harmonics.

2. Core Loss Analysis of Linear Magnetic Gear

2.1. Analysis Model of Linear Magnetic Gear

Figure 2 shows the shape and test bed of the linear magnetic gear used in this study.

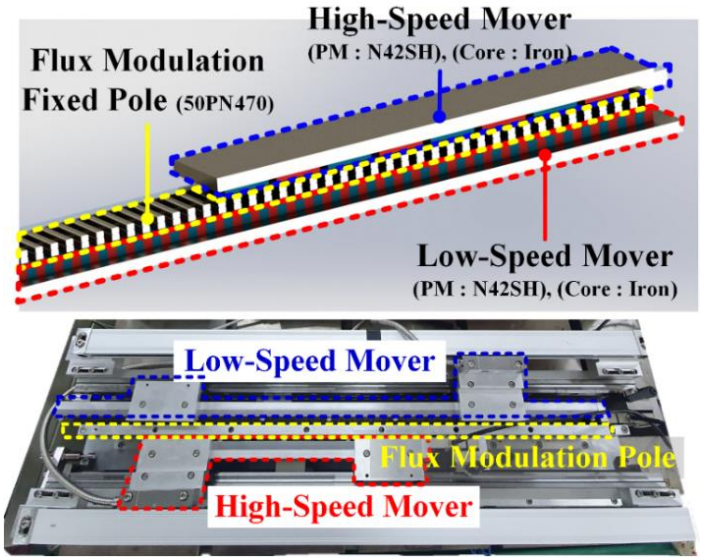

Figure 2. Structure and prototype of the linear magnetic gear.

Magnetic gears have permanent magnets attached to both their movers, and a magnetic flux modulation fixed-pole is located between the inner and the outer movers. The flux modulation fixed-pole modulates the magnetic field by the permanent magnet of the mover and the rotating magnetic field of the flux modulation fixed-pole, to produce a harmonic component corresponding to the pair number of low speed mover poles to have the characteristics of the gear [7]. The number of flux modulation fixed poles of a magnetic gear could be calculated by using the number of poles of the inner and outer permanent magnets, which could be calculated by Equation (1) [8].

$$F_{pole} = P_{low} + P_{high} \tag{1}$$

F_{pole} is the number of for flux modulation fixed-pole cores, and P_{low} and P_{high} are the number pole pairs of high-speed and low-speed mover permanent magnets. The designed gear has 8 poles of high-speed mover permanent magnets and 46 poles of low-speed mover permanent magnets, but if you calculate the number of flux modulation fixed poles with a pair of poles, it was calculated to be 27ea. In addition, the gear ratio (G_r) of the gear could be calculated by the number of poles of the high-speed mover and low-speed mover permanent magnets, which is shown in Equation (2) [9].

$$G_r = \frac{P_{low}}{P_{high}} \tag{2}$$

The gear ratio calculated through Equation (2) was 5.75. Then, by calculating the gear ratio of the magnetic gear, the moving speed of each mover can be calculated, using Equation (3).

$$\omega_{out} = -\frac{\omega_{in}}{G_r} \tag{3}$$

ω_{high} and ω_{low} refer to the speed of high- and low-speed movers. Since the high-speed mover speed of the designed linear magnetic gear is driven at 1 m/s, the moving speed of the low-speed mover calculated through Equation (3) is about -0.174 m/s. At this time, the negative sign in Equation (3) is because both movers rotate in opposite directions through the modulated magnetic field.

The linear magnetic gear designed in this study uses the NdFeB permanent magnet material with high magnetic energy, in order to deliver efficiency and force characteristics that are close to those of mechanical gears. However, such high magnetic energy causes

tensile stress and shear stress between the permanent magnet and the magnetic flux modulating iron core, on both sides of the linear magnetic gear.

Since this force can cause deformation of the linear magnetic gear, the core material of each mover was made of iron with excellent rigidity. For the flux modulation fixed-pole, 50PN470 electrical steel sheet manufactured by POSCO was used. Electrical steel sheet has a disadvantage of lower rigidity than iron, but has an advantage that is superior to iron in terms of loss, due to a low eddy current. Then, based on the magnetic flux density generated when the high-speed mover moved at 1 m/s and the low-speed mover was at −0.174 m/s, the core-loss analysis in each core was performed. The design specifications are as shown in Table 1.

Table 1. Design specifications of the linear magnetic gear.

Parameters	Value
High-speed mover length	322 mm
Low-speed mover length	702 mm
Thickness of low-speed core	10 mm
Thickness of low-speed mover permanent magnet	8 mm
Thickness of air-gap	2 mm
Thickness of flux modulation fixed-pole	9 mm
Thickness of high-speed core	10 mm
Thickness of high-speed mover permanent magnet	8 mm
High-speed mover number of poles	8
Low-speed mover number of poles	46
Moving speed of high-speed mover	1 m/s
Gear ratio	5.75

2.2. Coreloss Characteristic Equation

Electromagnetic losses include core-losses consisting of hysteresis losses and eddy current losses. Core-loss generates a magnetic field that changes in the positive and negative directions over time in the iron core when the AC power of the electric device was applied. Heat was generated due to this effect, which is called hysterical loss. In addition, the eddy current loss was linked to the iron core when the alternating magnetic field in the iron core changed with time, thereby generating organic electromotive force. This is a principle according to Faraday's law, where heat is generated due to organic electromotive force, and the heat loss that occurs at this time is called the eddy current loss. If this is expressed as an equation, it can be calculated by the Steinmetz equation, as shown in Equation (4) [10].

The core-loss (P_c) comprises the hysteresis loss (P_h) caused by the time-varying magnetic field and the eddy current loss (P_e) caused by the conductivity of the iron core. It can be seen that P_c is proportional to the frequencies f and B^n, and P_e is proportional to f^2 and B^2.

$$P_c = P_h + P_e = k_h f\ B^n + k_e f^2 B^2 \tag{4}$$

Here, f is the frequency of the magnetic field, B is the magnetic flux density of the iron core by the permanent magnet. k_h and k_e are the hysteresis loss and eddy current loss coefficients, respectively, n is the Steinmetz constant. However, the Steinmetz core-loss characteristic equation in Equation (4) is applied under the assumption that the magnetic flux density of the core is not saturated and the hysteresis loop is linear.

Therefore, the magnetic flux density in the iron core is 1 T or more, or a large error occurs in a high-frequency region. In addition to the hysteresis loss and eddy current loss components, an anomalous eddy current loss component was generated by the microscopic magnetic domain width or tension, such as structural changes in the material. Therefore, in order to accurately analyze the core-loss, it must be considered in Equation (4).

Considering the anomalous current loss in Equation (4) by Bertotti, it could be expressed in the modified Steinmetz equation, as shown in Equation (5).

$$P_c = P_h + P_e + P_a = k_h f B^n + k_e f^2 B^2 + k_a f^{1.5} B^{1.5} \quad (5)$$

Here, P_a is the anomalous eddy current loss, and k_a is the anomalous eddy current loss coefficient [11,12]. Since the anomalous eddy current loss could vary in the thickness, cross-sectional area, and conductivity of the material, the magnetic flux density was more than 1.5 T or the anomalous eddy current loss was considered in a high-frequency range, so more accurate core-loss analysis was possible. The size of the core-loss coefficient varied, based on the iron core material, and the size of the core-loss coefficient changed nonlinearly with frequency.

Therefore, it was crucial to obtain the precise values of the core-loss coefficients, such as k_h, k_e, and k_a in Equation (5), when predicting the use of the analytical method for core-loss. Core-loss data are mainly provided by manufacturers with products, and the difference in core-loss varies, depending on the frequency. Therefore, in this study, the curve fitting method was used to calculate the correct core-loss frequency. In order to calculate the core-loss coefficient for the unit frequency, the Steinmetz equation was divided by the frequency, as shown in Equation (6).

$$\frac{P_c}{f} = \frac{P_h + P_e + P_a}{f} = k_h B^n + k_e f B^2 + k_a f^{0.5} B^{1.5} \quad (6)$$

Figure 3 shows the result of calculating the core-loss coefficient for each frequency by substituting the core-loss data provided by the manufacturer into Equation (6) and comparing it with the measured core-loss value for each frequency. At this time, the hysterical loss coefficient, eddy current loss coefficient, and anomalous eddy current loss coefficient according to each frequency were calculated, as shown in Table 2.

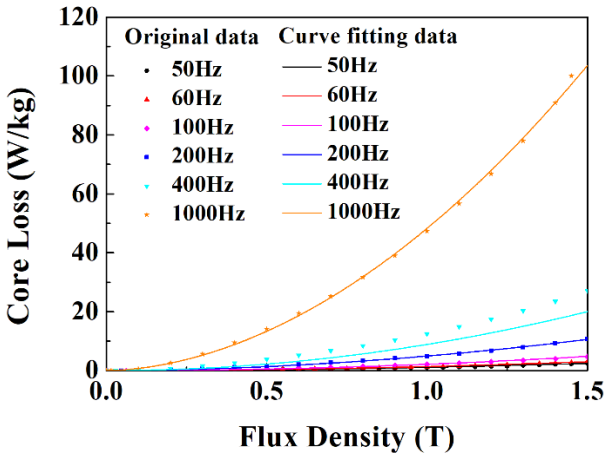

Figure 3. Curve fitting according to the core-loss material frequency.

Table 2. Core-loss coefficient according to frequency.

Frequency	k_h [w/kg]	k_e [w/kg]	k_a [w/kg]
50 [Hz]	0.018721	0.000458748	1.39192×10^{-5}
60 [Hz]	0.0188188	0.000458518	1.38762×10^{-5}
100 [Hz]	0.0216049	0	0
200 [Hz]	0.0150994	0.000461586	1.56562×10^{-5}
400 [Hz]	0.0162534	0.000465451	1.49788×10^{-5}
1000 [Hz]	0.0217835	0.000391975	1.4123×10^{-5}

2.3. Magnetic Field Behavior Analysis

In the literature of the core-loss analysis previously studied, it was confirmed through an experiment that the amount of core-loss generated in the alternating magnetic field and the rotating magnetic field differed about twice as much, based on the same magnetic flux density. Therefore, magnetic field behavior analysis is very important in core-loss analysis. The magnitude of the core-loss varies according to the magnetic field behavior characteristics, and the magnetic flux density generated by the harmonics increases the core-loss, so for accurate core-loss prediction, an accurate core-loss analysis should be performed by considering the harmonics and the magnetic field behavior [13]. Therefore, in order to increase the precision of the core-loss analysis, each analysis area was subdivided and calculated for magnetic field behavior analysis, and magnetic flux density analysis of linear magnetic gears through FEM. In addition, by performing FFT analysis on the derived magnetic flux density, the harmonics contained in the magnetic field were analyzed. The more subdivided the analysis model, the more accurate data on the magnetic field behavior and magnetic flux density in each region could be obtained, and thus more accurate core-loss analysis was possible. However, the number of subdivisions of the analysis model depended a lot on the experience of the designer for analysis time and accurate analysis results. Figure 4 shows the subdivided shape of each analysis area of the linear magnetic gear. The high-speed mover core was subdivided into 644 pieces, the flux modulation fixed-pole was subdivided into 432 pieces, and the low speed mover core was subdivided into 936 pieces. Figure 5 shows the results of the normal component and tangential component magnetic flux density analysis at arbitrary points (1-29, 1-504, 2-70, 2-75, 3-38, 3-499) in each region. Figure 6 shows the definition of the axis ratio for magnetic field behavior analysis. The definition of the axial ratio could be classified into a rotating magnetic field and an alternating magnetic field, by the ratio of the maximum and minimum values of the magnetic flux density of each component of the magnetic flux density in the vertical direction and the magnetic flux density in the tangential direction [14,15]. The alternating magnetic field has the characteristic of changing only the direction of the magnetic pole, and a rotating magnetic field meant that the magnetic field completes rotations. Therefore, when the ratio of the minor axis to the major axis was less than 0.1, the direction of magnetization was classified into an alternating magnetic field in which the direction of magnetization was not largely rotated in space but mainly changed in size in one direction, and when the ratio of the minor axis to the major axis was greater than 0.1, it was classified as a rotating magnetic field in which the size and direction changed together.

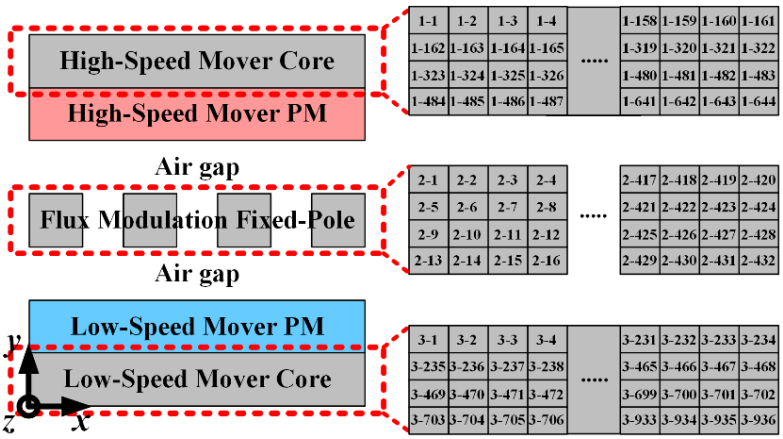

Figure 4. Segmentation analysis of core area.

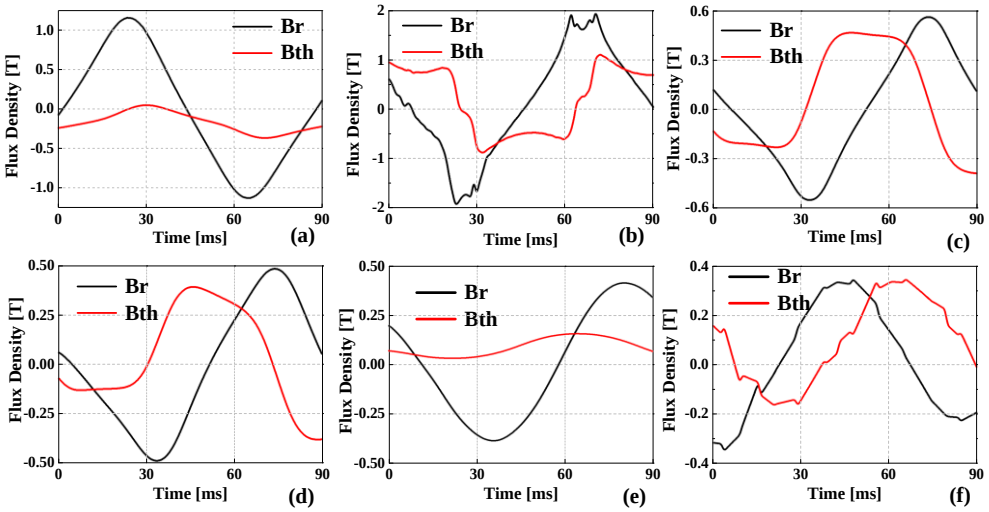

Figure 5. Magnetic flux density distribution in each subdivision area: (**a**) point 1-29, (**b**) point 1-504, (**c**) point 2-70, (**d**) point 2-75, (**e**) point 3-38, and (**f**) point 3-499.

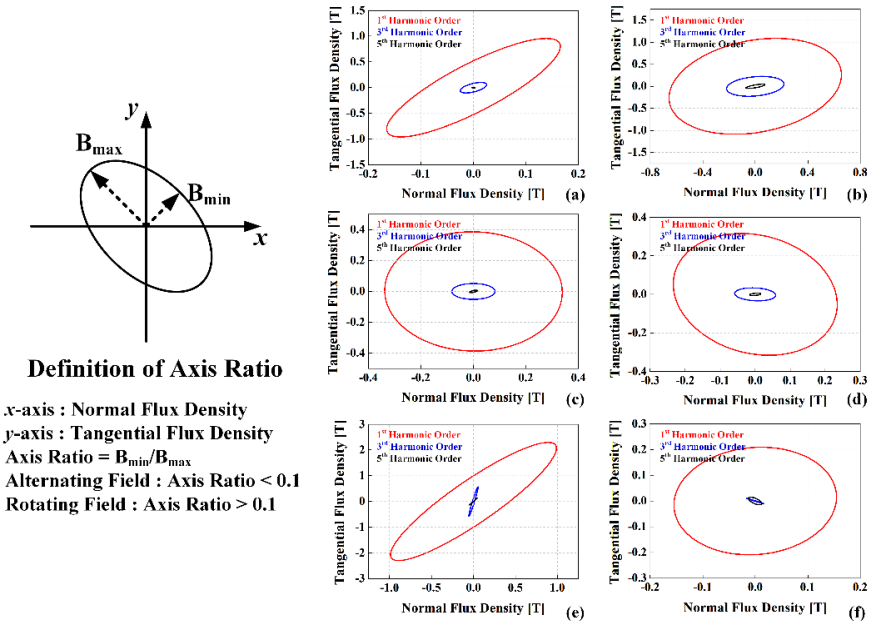

Figure 6. Analysis of the behavior of the magnetic field in each segmentation area: (**a**) point 1-29; (**b**) point 1-504; (**c**) point 2-70; (**d**) point 2-75; (**e**) point 3-38; and (**f**) point 3-499.

Figure 6 shows the magnetic field behavior of the first, third, and fifth harmonics derived from the magnetic flux density of the normal and tangential magnetic flux components at an arbitrary point (1-29, 1-504, 2-70, 2-75, 3-38, and 3-499) in the core region, separately. Points 1-504, 2-70, 2-75, and 3-38 indicate the rotating magnetic field because the axial ratio of the first harmonic component exceeded 0.1. In addition, points 1-29 and 3-38 yielded the result of the alternating magnetic field because the axial ratio of the first harmonic component was less than 0.1. The modified Steinmetz equation considering the magnetic flux density, based on the harmonic order, enabled a more accurate core-loss calculation using Equation (7).

$$P_c = \sum_{l=1,\,odd}^{\infty} k_{hl} f_l B_l^n + k_{el} f_l^2 B_l^2 + k_{al} f_l^{1.5} B_l^{1.5} \tag{7}$$

When the magnetic flux density of the core-loss was the same, the rotational magnetic field generated twice as much core-loss, as compared to the alternating magnetic field. Therefore, the final core-loss equation considering the magnetic field behavior analysis of each region could be calculated using Equation (8) [16]. Where l represents the harmonic order, and α is a constant, accounting for the rotating magnetic field. It has a value of 1 in an alternating magnetic field and 2 in a rotating magnetic field. α compensates for the inaccuracy of the core-loss coefficients derived, based on the Epstein data.

$$P_c = \sum_{l=1,odd}^{\infty} \alpha \left(k_{hl} f_l B_l^n + k_{el} f_l^2 B_l^2 + k_{al} f_l^{1.5} B_l^{1.5} \right) \quad \left\{ \begin{array}{l} \alpha = 1, \, alt.field \\ \alpha = 2, \, rot.field \end{array} \right\} \tag{8}$$

Figure 7 shows the core-loss calculated using the modified Steinmetz equation, in consideration of the alternating magnetic field and the magnetic flux density of the harmonic component and the core-loss result analyzed through FEM. The total core-loss obtained through the modified Steinmetz equation and FEM was 561.08 mW and 512.4 mW, respectively, and the core-loss derived through the two methods showed a difference of about 48.68 mW. At this time, the reason why the core-loss value of the FEM was lower was because the alternating and rotating magnetic fields were not considered, so a lower result was obtained.

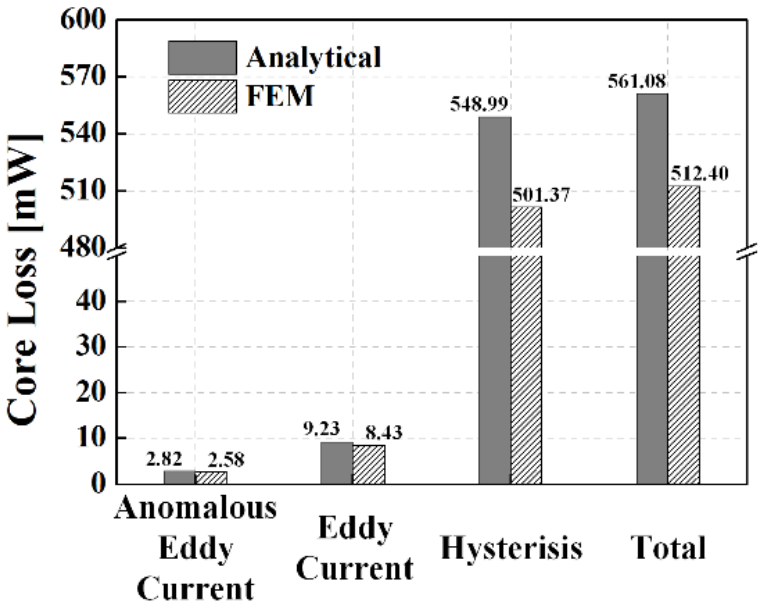

Figure 7. Modified Steinmetz equation and FEM core-loss comparison results.

3. Conclusions

Core-loss comprises hysteresis, eddy current, and anomalous eddy current losses, due to time varying magnetic fields. It is difficult to accurately interpret core-loss owing to the harmonics of the magnetic flux density in the core and the magnetic field behavior. However, in this study, the core-loss coefficient function of the equation was derived through the modified Steinmetz equation using curve fitting, based on the core-loss data provided by the manufacturer, and then the core-loss analysis of the linear magnetic gear was performed.

Then, through the modified Steinmetz equation, the final derived core-loss in consideration of the harmonics and magnetic field behavior and the derived core-loss using FEM were compared. As a result of the comparison, by substituting the magnetic flux density values of the alternating magnetic field, the rotating magnetic field, and the harmonic com-

ponent into Equation (6), Equation (7) was derived, and the modified Steinmetz equation based on this, resulted in a higher core-loss value.

In general, an experiment for measuring core-loss of an electric device is difficult, because it is difficult to obtain accurate data according to the characteristics of nonlinear materials. Accordingly, in many studies, reliability verification was performed by comparing the electromagnetic characteristics and efficiency of the device [15]. Figure 8 shows the comparison result of FEM and the experimental characteristics of the manufactured linear magnetic gear. As a result of the comparison of the experimental measurements, the error was about 2.3%, and the displacement amount and the measured speed of each mover over time were well-matched to the gear ratio of 5.75. In addition, the load analysis results of the linear magnetic gear are shown in Table 3, and the output of about 54 W was derived. As a result of comparing the core-loss derived through the modified Steinmetz equation and the core-loss of the conventional analysis method, an error rate of about 9.5% was obtained, and the total loss increased by 1.3% due to this error. As the total loss increased, the efficiency of the gear using the modified Steinmetz equation was reduced, as compared to the core-loss efficiency calculated through FEM.

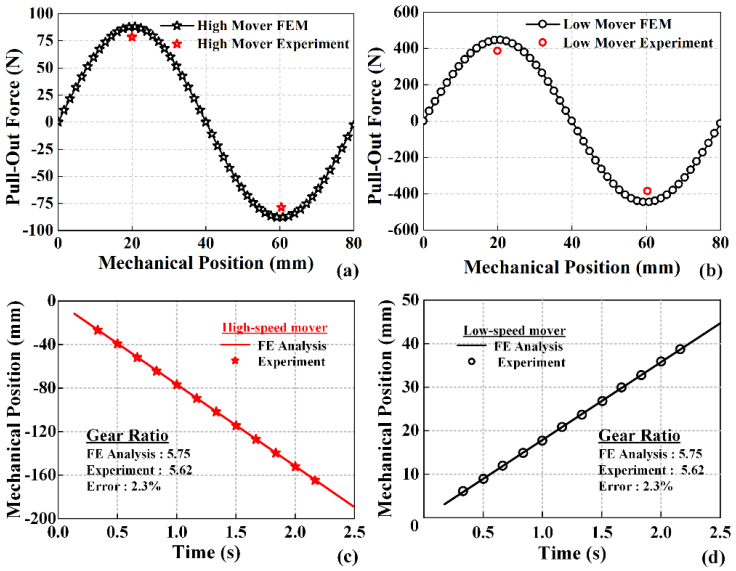

Figure 8. FEM and experiment comparison results—(**a**) Pull-out force of the high-speed mover, (**b**) pull-out force of the low-speed mover, (**c**) displacement amount of the high-speed mover, and (**d**) displacement amount of the low-speed mover.

Table 3. Analysis results of the linear magnetic gear.

Parameters	Modified Steinmetz Core-Loss	FEM Core-Loss
Input Power [W] (high-speed mover)	58.4	58.1
Output Power [W] (low-speed mover)	54.65	54.41
Solid Loss [W]	3.18	
Core-Loss [mW]	561.08	512.405
Efficiency [%]	93.59	93.64

Therefore, it was considered that the core-loss analysis using the modified Steinmetz equation presented in this paper could analyze the electromagnetic performance characteristics, considering the more accurate core-loss than the core-loss derived through FEM.

Author Contributions: J.-Y.C.; conceptualization, review, and editing, J.-I.L.; original draft preparation, analysis, and experiment, K.-H.S.; core-loss analysis through analytical method, T.-K.B.; co-simulation, K.-Y.H.; co-simulation, K.-H.K.; co-simulation and experiment. All authors have read and agreed to the published version of the manuscript.

Funding: This research was supported by Korea Electric Power Corporation. (Grant number: R20XO02-38).

Institutional Review Board Statement: Not applicable.

Informed Consent Statement: Not applicable.

Conflicts of Interest: The authors declare no conflict of interest.

References

1. Gardner, M.C.; Johnson, M.; Toliyat, H.A. Analysis of High Gear Ratio Capabilities for Single-Stage, Series Multistage and Compound Differential Coaxial Magnetic Gears. *IEEE Trans. Energy Convers.* **2019**, *34*, 665–672. [CrossRef]
2. Shin, H.M.; Chang, J.H. Comparison of Radial Force at Modulating Pieces in Coaxial Magnetic Gear and Magnetic Gear Machine. *IEEE Trans. Magn.* **2018**, *54*, 1–4. [CrossRef]
3. Tlalim, P.M.; Gerber, S.; Wang, R.-J. Optimal Design of an Outer-Stator Magnetically Geared Permanent Magnet Machine. *IEEE Trans. Magn.* **2016**, *52*, 1–10. [CrossRef]
4. Frandsen, T.V.; Mathe, L.; Berg, N.I.; Holm, R.K. Motor Integrated Permanent Magnet Gear in a Battery Electrical Vehicle. *IEEE Trans. Ind. Appl.* **2015**, *51*, 1516–1525. [CrossRef]
5. Park, E.J.; Jung, S.Y.; Kim, Y.J. Comparison of Magnetic Gear Characteristics Using Different Permanent Magnet Materials. *IEEE Trans. Appl. Supercond.* **2020**, *30*, 1–4. [CrossRef]
6. Nam, H.; Ha, K.H.; Lee, J.J.; Hong, J.P.; Kang, G.H. A Study on Iron Loss Analysis Method Considering the Harmonics of the Flux Density Waveform Using Iron Loss Curves Tested on Epstein Samples. *IEEE Trans. Magn.* **2003**, *39*, 1472–1475. [CrossRef]
7. Göbl, E.; Jungmayr, G.; Marth, E.; Amrhein, W. Optimization and Comparison of Coaxial Magnetic Gears with and without Back Iron. *IEEE Trans. Magn.* **2018**, *54*, 1–4. [CrossRef]
8. Gardner, M.C.; Johnson, M.; Toliyat, H.A. Comparison of Surface Permanent Magnet Axial and Radial Flux Coaxial Magnetic Gears. *IEEE Trans. Energy Convers.* **2018**, *33*, 2250–2259. [CrossRef]
9. Johnson, M.; Gardner, M.C.; Toliyat, H.A.; Ouyang, W.; Tschida, C. Design, Construction, and Analysis of a Large-Scale Inner Stator Radial Flux Magnetically Gear Generator for Wave Energy Conversion. *IEEE Trans. Ind. Appl.* **2018**, *54*, 3305–3314. [CrossRef]
10. Zhu, Z.Q.; Ng, K.; Schofield, N.; Howe, D. Analytical Prediction of Rotor Eddy Current Loss in Brushless Machines Equipped with Surfaced-Mounted Permanent Magnets, Part II: Accounting for Eddy Current Reaction Field. In Proceedings of the Fifth International Conference in Electrical Machines and Systems, Shenyang, China, 18–20 August 2001; Volume 2, pp. 810–813. [CrossRef]
11. Steinmetz, C. On the Law of Hysteresis. *IEEE Trans. Am. Inst. Electr. Eng.* **1892**, *9*, 1–64. [CrossRef]
12. Yamazaki, K.; Fukishima, N. Iron Loss Model for Rotating Machine: Comparison between Bertotti's Three Term Expression and 3-D Eddy Current Analysis. *IEEE Trans. Magn.* **2010**, *46*, 3121–3124. [CrossRef]
13. Kim, C.W.; Koo, M.M.; Kim, J.M.; Ahn, J.H.; Hong, K.Y.; Choi, J.Y. Core Loss Analysis of Permanent Magnet Synchronous Generator with Slotless Stator. *IEEE Trans. Appl. Supercond.* **2018**, *28*, 1–4. [CrossRef]
14. Enokizono, M.; Suzuki, T.; Sievert, J.; Xu, J. Rotational Power Loss of Silicon Steel Sheet. *IEEE Trans. Magn.* **1990**, *26*, 2562–2564. [CrossRef]
15. Kim, C.W.; Kim, J.M.; Seo, S.W.; Ahn, J.H.; Hong, K.Y.; Choi, J.Y. Core Loss Analysis of Permanent Magnet Linear Synchronous Generator Considering the 3-D Flux Path. *IEEE Trans. Magn.* **2018**, *54*, 1–4. [CrossRef]
16. Woo, J.H.; Kim, C.W.; Bang, T.K.; Lee, S.H.; Lee, K.S.; Choi, J.Y. Experimental Verification and Electromangetic Characteristic Analysis of Permanent Magnet Linear Oscillating Actuator Using Semi 3D Analysis Technique with Corrected Stacking Factor. *Trans. Appl. Supercond.* **2020**, *30*, 1–4. [CrossRef]